Approximating long-term statistics early in the Global Precipitation Measurement era

Thomas Stanley

Universities Space Research Association, Columbia, Maryland, USA

Goddard Earth Sciences Technology and Research, Columbia, Maryland, USA

Hydrological Sciences Laboratory, Goddard Space Flight Center, Greenbelt, Maryland, USA

Dalia B. Kirschbaum, Corresponding Author

Hydrological Sciences Laboratory

Goddard Space Flight Center

8800 Greenbelt Road

Greenbelt, Maryland, USA

301.614.5810

dalia.b.kirschbaum@nasa.gov

George J. Huffman

Mesoscale Atmospheric Processes Laboratory, NASA Goddard Space Flight Center, Greenbelt, Maryland

Robert F. Adler

Earth System Sciences Interdisciplinary Center, University of Maryland, College Park, College Park, Maryland

Abstract

Long-term precipitation records are vital to many applications, especially the study of extreme events. The Tropical Rainfall Measuring Mission (TRMM) has served this need, but TRMM's successor mission, Global Precipitation Measurement (GPM), does not yet provide a long-term record. Quantile mapping, the conversion of values across paired empirical distributions, offers a simple, established means to approximate such long-term statistics, but only within appropriately defined domains. This method was applied to a case study in Central America, demonstrating that quantile mapping between TRMM and GPM data maintains the performance of a real-time landslide model. Use of quantile mapping could bring the benefits of the latest satellite-based precipitation dataset to existing user communities such as those for hazard assessment, crop forecasting, numerical weather prediction, and disease tracking.

1   Introduction

2   Many users of precipitation data require long-term records, especially when characterizing

3   extreme events. Satellite-based precipitation estimates can meet this need in locations without

4   dense gauge networks. The National Aeronautics and Space Administration (NASA) has been

5   providing near real-time precipitation data to the community since 2002 (Huffman et al. 2010,

6   2007). The Tropical Rainfall Measurement Mission (TRMM) was launched in November, 1997.

7   Its successor, the Global Precipitation Measurement (GPM) Core Observatory, was launched in

8   February 2014 and extends observations of both falling snow and heavy to light rain past 65˚N-

9   S (Hou et al. 2014). To provide nearly global coverage with short revisit times, the TRMM and

10   GPM missions rely on a constellation of partner satellites. The TRMM Multi-satellite

11   Precipitation Analysis (TMPA) covers the area from 50˚N-S from 2000-present (Table 1), while

12   the Integrated Multi-satellitE Retrievals for GPM (IMERG) covers 60˚N-S from March 2014-

13   present (Huffman et al. 2015).

14

15   Due to the use of different sensors, algorithms, and calibrations, the IMERG and TMPA products

16   differ considerably. A comparison of percentiles from 7 March 2015 to 6 March 2016 for the

17   GIS-formatted IMERG Version 3 Late run (IMERG-L) and Real-time TMPA Version 7 (TMPA-RT)

18   daily products (Huffman 2016a,b) revealed some of the characteristics of these differences

19   (Figure 1). Days with zero estimated precipitation were included in the distribution because

20   TMPA-RT and IMERG-L differ in the ability to detect very light precipitation (Hou et al. 2014). At

21   specific percentiles, the TMPA-RT values were resampled to a 0.1° grid by the nearest neighbor

22   method, then the IMERG-L values were subtracted. At the 75th percentile (Fig 1a), there are

23   small differences between TMPA-RT and IMERG-L, but differences of more than 100 mm day^{-1}

24   at the 95th percentile (Fig 1b). TMPA-RT tends to show heavier tropical precipitation (blue), and

25   IMERG-L tends to show heavier mid-latitude precipitation (red). In particular, the southern

26   ocean shows a large and relatively consistent difference between IMERG-L and TMPA-RT.

27   However, many locations do not fit this pattern, including some mountains and inland water

28   bodies. In addition to geographic heterogeneity, the relationship between TMPA-RT and

29   IMERG-L may vary seasonally and interannually. Combined, these factors complicate the use of

30   IMERG data in TMPA-based applications.

31

32   Satellite precipitation data are used in many applications such as flood monitoring, crop

33   forecasting, numerical weather prediction, and disease tracking (Kucera et al. 2013; Kirschbaum

34   et al. 2016). These user communities have relied upon TMPA data, and several workshops have

35   highlighted the need for long precipitation records (Ward et al. 2015; Ward and Kirschbaum

36   2014). While the GPM mission plans to create a consistent record of precipitation available

37   from 1998 to the present using TRMM, GPM, and partner data, this processing is not planned to

38   begin before 2018. Until that happens, application developers could take advantage of IMERG's

39   improved spatial and temporal resolution and accuracy while maintaining the benefits of

40   TMPA's long time series by adapting IMERG data to TMPA-equivalent values with quantile

41   mapping. Quantile mapping (also known as quantile matching, cumulative distribution function

42   [CDF] matching, etc.) has been used to convert gridded precipitation data to its point-based

43   equivalent (Gudmundsson et al. 2012), to adapt gridded precipitation data to a different spatial

44 resolution (Maraun 2013), and to correct model bias at the same resolution as observational

45 data (Cannon et al. 2015). Gudmundsson et al. (2012) recommended the use of nonparametric

46 data transformations (e.g. empirical quantiles) for reducing biases across the entire distribution,

47 so these methods may be more appropriate for transforming extreme values such as rainfall

48 thresholds. An example of the statistical transformation of an empirical rainfall distribution can

49 be found in the second chapter of Some Applications of Statistics to Meteorology (Panofsky and

50 Brier 1968).

51

52 To demonstrate the use of IMERG in a TMPA-based application, quantile mapping from TMPA-

53 RT to IMERG-L was applied to the Landslide Hazard Assessment for Situational Awareness

54 (LHASA) model. LHASA issues a daily nowcast with a resolution of approximately 1 kilometer

55 (Kirschbaum et al. 2015a). The nowcast includes both a moderate-hazard level to maximize

56 sensitivity and a high-hazard level to reduce the number of false alarms. LHASA combines

57 rainfall and landslide susceptibility with a heuristic decision tree. First, areas rated "very low"

58 on the Landslide Susceptibility Map of Central America and the Caribbean Islands (Kirschbaum

59 et al. 2015b) are excluded from further analysis. Second, a 60-day antecedent rainfall index is

60 calculated from TMPA-RT. Third, the current daily rainfall accumulation is compared to 1 of 2

61 climatological thresholds, depending upon the level of antecedent rainfall. LHASA was

62 calibrated over the period 2007-2013 with reference to the Global Landslide Catalog (GLC), an

63 inventory of rainfall-triggered landslides reported by media and other sources (Kirschbaum et

64 al. 2015c, 2010). LHASA was validated by the GLC events occurring in 2014.

65

Methods

67   LHASA was developed and calibrated with TMPA-RT precipitation estimates, but the transition

68   from TRMM to GPM required that the model be updated to use IMERG-L inputs, which do not

69   currently have the long record needed for development of the necessary rainfall-landslide

70   relations. The quantile mapping technique was accomplished in four main steps: 1) evaluation

71   of data time series and characteristics, 2) selection of space-time domain, 3) quantile

72   calculations, and 4) quantile mapping through LHASA case study. Nearly 17 years of TMPA-RT

73   and 1.2 years of IMERG-L were available for this case study.

74

75   First, the characteristics of each dataset were considered. Both products are produced at a

76   moderate spatial resolution, but the finer resolution of IMERG-L is associated with higher

77   precipitation estimates for extreme events, as expected. Land and sea pixels exhibit distinct

78   rainfall patterns in both IMERG-L and TMPA-RT. The relationship between products is spatially

79   heterogeneous on land (Figure 1), is not controlled solely by elevation, and is likely to be

80   difficult to predict on the basis of other variables.

81

82   Second, the selection of a space-time domain on which to perform quantile mapping is

83   necessarily a compromise between sample size and the relevance of the empirical distributions

84   to a specific time and place (Reichle and Koster 2004; Voisin et al. 2010). The short time period

85   for which IMERG-L is available, combined with the relatively homogeneous time series,

86   suggested that calculation of separate monthly quantiles would reduce the sample size, without

87   making the data transformation much more representative of each month. Therefore, all data

88   from 6 May 2015 to 5 May 2016 were assigned to the same domain. Spatial heterogeneity of

89   precipitation estimates across the region implied that it would be beneficial to partition the

90   data before quantile mapping, but the absence of strong ties between the difference maps and

91   elevation, land cover, or standard climate zones made it difficult to do so on an a priori basis.

92   More importantly, LHASA focuses on extreme rainfall events. This upper tail of the distribution

93   is best described by a large sample. Therefore, the entire land area was assigned to single

94   domain. Marine pixels were not included, because these are not representative of rainfall on

95   land.

96

97   Third, 100,000 quantiles were calculated for the TMPA-RT and IMERG-L products in the

98   statistical software R (R Core Team 2015; Hijmans 2015). The large number of quantiles (1

99   cutpoint for every 0.001% of each distribution) approximated the empirical CDF and minimized

100   the error associated with interpolation of extreme rainfall. Then the quantiles for IMERG-L and

101   TMPA-RT were paired into a single table that described the whole land area over 1 year. Fourth,

102   the table was applied to each LHASA daily rainfall threshold (based on TMPA-RT) to produce

103   equivalent IMERG-L thresholds (Figure 2). These four steps were repeated for values of the 60-

104   day antecedent rainfall index.

105

106   Fourth, the quantile-mapped version of LHASA was run with IMERG-L data. The performance of

107   the adapted rainfall thresholds was evaluated by a comparison to the original TMPA-based

108   model. The true positive rate (TPR) was determined by calculating the proportion of reported

109   landslide events (GLC) that were predicted correctly by LHASA. There may be some error in the

110   reported dates of GLC events (Kirschbaum et al. 2015c). To address this issue, TPR was

111   calculated for 1-day, 3-day, and 7-day windows (e.g. if LHASA correctly predicted a landslide

112   that occurred 2 days before its reported date, it would be counted as a true positive only for

113   the 7-day window). The number of pixel-days for which a nowcast was issued without a GLC

114   event were divided by the total number of pixel-days to determine the false positive rate (FPR).

115   These results were also compared to the LHASA calibration period.

116

Results

118   In general, the version of LHASA with IMERG-adapted thresholds remained very similar to the

119   TMPA version. Figure 3 shows the TMPA rainfall thresholds (a) and the new IMERG thresholds

120   (b). The magnitude of the change was greatest in the wettest locations due to differences in

121   calibration, the shift to finer resolution, or both. Model performance with IMERG-L was

122   comparable to TMPA-RT for both the high-hazard and moderate-hazard nowcasts (Table 2). The

123   FPR was consistent across inputs, due to the fact that quantile mapping maintains the

124   frequency with which a threshold will be exceeded. Although better results were obtained

125   during the model calibration period (2007-2013), TMPA-RT and IMERG-L produced comparable

126   postcalibration performance.

127

128 Although the overall performance was good (Table 2), the high-hazard model run with IMERG-L

129 produced a FPR over 20% in San José, Costa Rica. The anomaly did not occur elsewhere and was

130 caused by the fact that the IMERG record shows unusually frequent and heavy rainfall in the

131 Costa Rican capital (Figure 4) compared to the nearby site of El Bosque, as well as the entire

132 region. Thus, the single Central American domain was not representative of the relationship

133 between IMERG and TMPA at this site, and quantile mapping did not correct the local bias.

134

135 ## Discussion

136 LHASA showed comparable performance for IMERG and TMPA inputs, which suggests that

137 quantile mapping successfully adapted the model to the new precipitation data stream. It is

138 anticipated that subsequent versions of IMERG will further improve the precipitation estimates,

139 particularly for extreme rainfall. However, performance varied locally. Anomalous locations

140 may be poorly served by quantile mapping across a single time-space domain. If the application

141 were focused on such a location, quantile mapping should be applied more locally.

142

143 In other study areas and for other applications, it may be appropriate to use a different quantile

144 mapping scheme. In cases where a large amount of data is available and the relationship

145 between TMPA and IMERG varies seasonally, it may be helpful to segment the data by month

146 or season before quantile mapping (e.g. Turkington et al. 2016; Wood et al. 2004). In cases with

147 little to no seasonal variation, it may be appropriate to include partial years in the precipitation

148   distribution. The land surface could be divided into elevation or climate zones, if these features

149   were consistently associated with biases in the precipitation data. In cases with a high degree of

150   spatial heterogeneity, it may be necessary to treat each pixel separately (e.g. Wood et al. 2004;

151   Voisin et al. 2010), which would require numerous data transformations and a sufficient

152   temporal record at each point. Another approach is to calculate quantiles within a spatial

153   sampling window (Reichle and Koster 2004). In some cases, there may be too little data that is

154   relevant to the research topic; these studies may require a more sophisticated approach than

155   quantile mapping.

156

Conclusions

158   Quantile mapping can adapt IMERG data for applications that were designed to use TMPA

159   precipitation estimates. In Central America, a daily landslide hazard model was adapted for use

160   with IMERG data by quantile mapping across a single domain. The results were comparable to

161   those for the original TMPA-based model. It is likely that other long-term precipitation datasets

162   would benefit from the same treatment. However, this method may be more successful with

163   threshold-based models and could be impacted by low sample size at the most extreme

164   precipitation values. Another key limitation of the method is that it must be applied over a

165   space-time domain with a consistent relationship between TMPA and IMERG. If this

166   requirement cannot be met, a more sophisticated treatment of the data may be required.

167   Ultimately, a longer IMERG record will obviate the need for this technique, because the user

168   community will be able to develop new climatological datasets directly from IMERG.

169

Acknowledgements

174

References

Cannon, A. J., S. R. Sobie, and T. Q. Murdock, 2015: Bias Correction of GCM Precipitation by

Quantile Mapping: How Well Do Methods Preserve Changes in Quantiles and Extremes? *J.*

Clim., **28**, 6938–6959, doi:10.1175/JCLI-D-14-00754.1.

http://journals.ametsoc.org/doi/full/10.1175/JCLI-D-14-00754.1# (Accessed May 2, 2016).

Gudmundsson, L., J. B. Bremnes, J. E. Haugen, and T. Engen Skaugen, 2012: Technical Note:

Downscaling RCM precipitation to the station scale using quantile mapping – a comparison

of methods. *Hydrol. Earth Syst. Sci. Discuss.*, **9**, 6185–6201, doi:10.5194/hessd-9-6185-

2012. http://www.hydrol-earth-syst-sci-discuss.net/9/6185/2012/.

Hijmans, R. J., 2015: raster: Geographic Data Analysis and Modeling. R package version 2.4-15.

http://cran.r-project.org/package=raster.

Hou, A. Y., and Coauthors, 2014: The Global Precipitation Measurement Mission. *Bull. Am.*

Meteorol. Soc., **95**, 701–722, doi:10.1175/BAMS-D-13-00164.1.

http://journals.ametsoc.org/doi/abs/10.1175/BAMS-D-13-00164.1.

189   Huffman, G. J., 2016a: GPM (IMERG) Late Precipitation L3 1 day 0.1 degree x 0.1 degree V03.

190   ftp://jsimpson.pps.eosdis.nasa.gov/ (Accessed May 24, 2016).

191   ——, 2016b: TRMM (TMPA) Real-Time Precipitation L3 1 day 0.1 degree x 0.1 degree V07.

192   ftp://trmmopen.gsfc.nasa.gov/pub/gis/ (Accessed July 17, 2016).

193   ——, and Coauthors, 2007: The TRMM Multisatellite Precipitation Analysis (TMPA): Quasi-

194   Global, Multiyear, Combined-Sensor Precipitation Estimates at Fine Scales. *J.*

195   *Hydrometeorol.*, **8**, 38–55, doi:10.1175/JHM560.1.

196   ——, R. F. Adler, D. T. Bolvin, and E. J. Nelkin, 2010: The TRMM Multi-satellite Precipitation

197   Analysis (TMPA). *Satellite Rainfall Applications for Surface Hydrology*, F. Hossain and M.

198   Gebremichael, Eds., Springer Verlag, 3–22.

199   ——, D. T. Bolvin, D. Braithwaite, K. Hsu, R. J. Joyce, and P. Xie, 2015: *Algorithm Theoretical*

200   *Basis Document (ATBD) for NASA Global Precipitation Measurement (GPM) Integrated*

201   *Multi-satellitE Retrievals for GPM (IMERG)*. 30 pp.

202   Kirschbaum, D. B., R. F. Adler, Y. Hong, S. Hill, and A. Lerner-Lam, 2010: A global landslide

203   catalog for hazard applications: Method, results, and limitations. *Nat. Hazards*, **52**, 561–

204   575, doi:10.1007/s11069-009-9401-4.

205   ——, T. Stanley, and J. Simmons, 2015a: A dynamic landslide hazard assessment system for

206   Central America and Hispaniola. *Nat. Hazards Earth Syst. Sci.*, **15**, 2257–2272,

207   doi:10.5194/nhess-15-2257-2015. http://www.nat-hazards-earth-syst-

208   sci.net/15/2257/2015/nhess-15-2257-2015.html (Accessed November 10, 2015).

209   ——, ——, and S. Yatheendradas, 2015b: Modeling Landslide Susceptibility over Large Regions

210   with Fuzzy Overlay. *Landslides*, doi:10.1007/s10346-015-0577-2.

211   http://link.springer.com/article/10.1007/s10346-015-0577-2.

212   ——, ——, and Y. Zhou, 2015c: Spatial and temporal analysis of a global landslide catalog.

213   *Geomorphology*, **249**, 4–15, doi:10.1016/j.geomorph.2015.03.016.

214   http://www.sciencedirect.com/science/article/pii/S0169555X15001579.

215   ——, and Coauthors, 2016: NASA's Remotely-sensed Precipitation: A Reservoir for Applications

216   Users. *Bull. Am. Meteorol. Soc.*, **In review**.

217   Kucera, P. A., E. E. Ebert, F. J. Turk, V. Levizzani, D. Kirschbaum, F. J. Tapiador, A. Loew, and M.

218   Borsche, 2013: Precipitation from space: Advancing earth system science. *Bull. Am.*

219   *Meteorol. Soc.*, **94**, 365–375, doi:10.1175/BAMS-D-11-00171.1.

220   http://journals.ametsoc.org/doi/full/10.1175/BAMS-D-11-00171.1.

221   Maraun, D., 2013: Bias Correction, Quantile Mapping, and Downscaling: Revisiting the Inflation

222   Issue. *J. Clim.*, **26**, 2137–2143, doi:10.1175/JCLI-D-12-00821.1.

223   http://journals.ametsoc.org/doi/abs/10.1175/JCLI-D-12-00821.1 (Accessed May 4, 2016).

224   R Core Team, 2015: R: A language and environment for statistical computing. http://www.r-

225   project.org/.

226   Reichle, R. H., and R. D. Koster, 2004: Bias reduction in short records of satellite soil moisture.

227   *Geophys. Res. Lett.*, **31**, doi:10.1029/2004GL020938.

228   http://onlinelibrary.wiley.com/doi/10.1029/2004GL020938/full.

229   Turkington, T., A. Remaître, J. Ettema, H. Hussin, and C. van Westen, 2016: Assessing debris

230   flow activity in a changing climate. *Clim. Change*, **0**, 1–16, doi:10.1007/s10584-016-1657-6.

231   http://link.springer.com/article/10.1007/s10584-016-1657-6.

232   Voisin, N., J. C. Schaake, and D. P. Lettenmaier, 2010: Calibration and Downscaling Methods for

233   Quantitative Ensemble Precipitation Forecasts. *Weather Forecast.*, **25**, 1603–1627,

234   doi:10.1175/2010WAF2222367.1.

235   Ward, A., and D. Kirschbaum, 2014: Measuring Rain for Society's Gain: GPM Applications

236   Workshop. *NASA Earth Obs.*, **26**, 4–11.

237   ——, ——, and M. Hobish, 2015: Measuring Rain and Snow for Science and Society: The Second

238   GPM Applications Workshop. *Earth Obs.*, **27**, 4–11.

239   Wood, A. W., L. R. Leung, V. Sridhar, and D. P. Lettenmaier, 2004: Hydrologic implications of

240   dynamical and statistical approaches to downscaling climate model outputs. *Clim. Change*,

241   **62**, 189–216, doi:10.1023/B:CLIM.0000013685.99609.9e.

242   http://link.springer.com/article/10.1023/B:CLIM.0000013685.99609.9e#enumeration.

243

244   Tables

245   *Table 1: Summary of TRMM and GPM multi-satellite products, resolutions, availability and*

246   *latency. The TRMM Level 3 multi-satellite product TMPA has a near real-time version that is*

247   *calibrated with a gauge climatology and a research product that uses a global network of*

248   *gauges to calibrate the product. GPM Level 3 IMERG has three versions: the early run is*

249   *produced with a latency of ~5 hours after satellite acquisition. The late run uses more satellite*

250   *information and an improved morphing scheme, and a final run uses a global gauge network to*

251   *calibrate the observations.*

Satellite	Algorithm Name	Resolution		Coverage	Available	Latency
		Space	*Time*			
TRMM	TRMM Multi-Satellite Precipitation Analysis (TMPA Version 7)	0.25° x 0.25°	3 hours	Gridded, 50°N-50°S	2000-present	8 hours (Real time)
					1998 to present	2 months (Research)
GPM	Integrated Multi-satellitE Retrievals for GPM (IMERG)	0.1° x 0.1°	30 minutes	Gridded, 65°N-65°S	April 2015-present	5 hours (Early run)
					March 2015-present	15 hours (Late run)
					March 2014-Present	3.5 months (Final run)

252

253   *Table 2: The performance of TMPA-RT and IMERG-L was compared by determining the number*

254   *of landslides predicted by each model run. This table shows: (a) precipitation product ; (b)*

255   *corresponding date range; (c) version of LHASA that was tested (d) number of landslides*

256   *reported during each time period; (e)-(g) proportion of landslides for which a nowcast was*

13

257   *issued on the reported date (1-day), the day before or after the reported event (3-day), and*

258   *within a 7-day window around the reported date, respectively; and (h) FPR or overall frequency*

259   *with which LHASA issues nowcasts at dates and places without recorded landslides.*

a. Model input	b. Date range of model run	c. Hazard Level	d. Landslide Reports	e. 1-day TPR	f. 3-day TPR	g. 7-day TPR	h. FPR
TMPA-RT	2007-2013	Moderate	99	64%	77%	83%	11%
TMPA-RT	2014	Moderate	43	58%	74%	79%	9%
TMPA-RT	5/2015-5/2016	Moderate	73	45%	73%	84%	6%
IMERG-L	5/2015-5/2016	Moderate	73	56%	73%	82%	10%
TMPA-RT	2007-2013	High	99	26%	37%	47%	1%
TMPA-RT	2014	High	43	12%	33%	47%	1%
TMPA-RT	5/2015-5/2016	High	73	15%	29%	37%	1%
IMERG-L	5/2015-5/2016	High	73	12%	40%	49%	1%

260

261

Figure Caption List

Figure 1: Difference between TMPA-RT (regridded to 0.1°) and IMERG-L from March 7, 2015 to

March 6, 2016 for the daily a) 75th and b) 95th percentiles. Positive values indicate areas where

TMPA-RT is higher (blue) and negative areas show that IMERG-L is higher (red). At these

percentiles, no difference was observed in many arid regions, but differences can be observed in
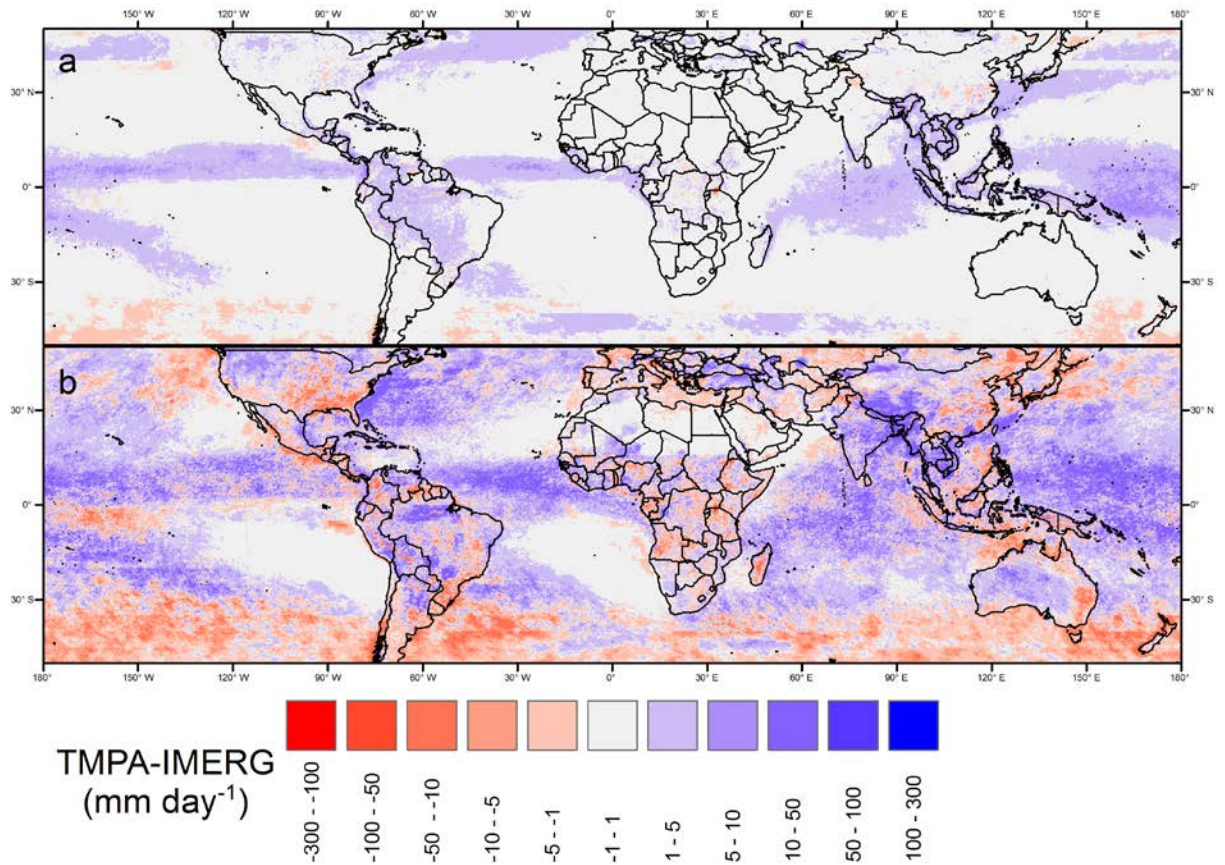
those regions during rare precipitation events.

Figure 2: Quantile-quantile plot for the Central American land area for May 6, 2015-May 5,

2015. 100,000 quantiles (open circles) were calculated for the TMPA-RT and IMERG-L rainfall

estimates. In quantile mapping, a value from one product is used to look up the value of the

second product at the same quantile. For example, if a TMPA-RT precipitation threshold were

180 mm day^{-1}, the equivalent IMERG-L value would be 231 mm day^{-1}.

Figure 3: (a) The LHASA high-hazard rainfall threshold was calculated from TMPA-RT data for

the period 2001-2014. (b) The quantile-mapped IMERG-L equivalent thresholds.

Figure 4: Quantile-quantile plot of two locations in Costa Rica, as well as the whole of Central

America (black). Dry days are not shown. El Bosque (blue) is separated from San José (red) by

approximately 45 kilometers, but the observed relationship between IMERG-L and TMPA-RT is

dramatically different. The capital of Costa Rica has an anomalous IMERG record, in which

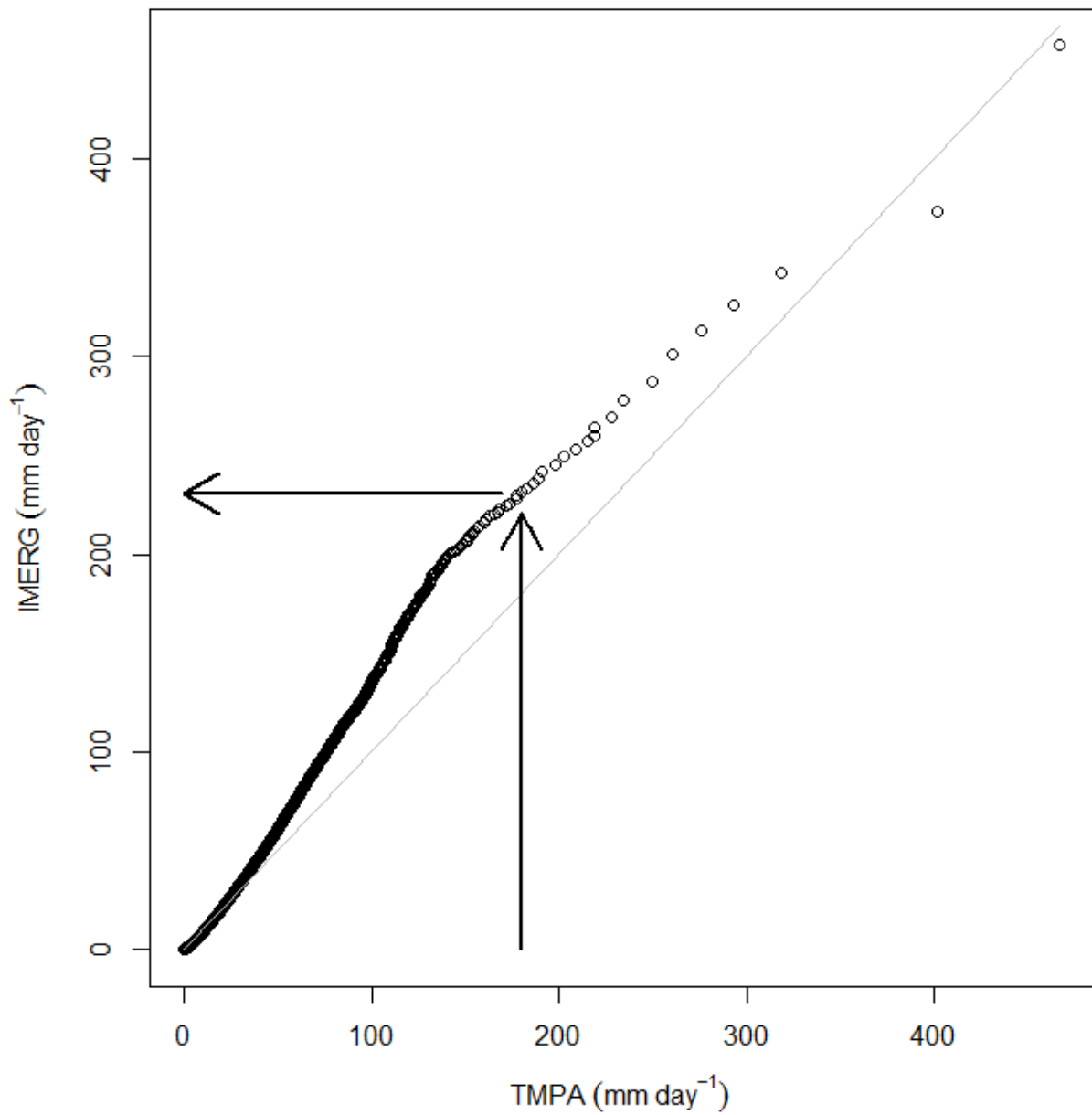*precipitation is both heavier and more frequent.*

281   Figures

282

Figure 1: Difference between TMPA-RT (regridded to 0.1°) and IMERG-L from March 7, 2015 to

March 6, 2016 for the daily a) 75th and b) 95th percentiles. Positive values indicate areas where

TMPA-RT is higher (blue) and negative areas show that IMERG-L is higher (red). At these

percentiles, no difference was observed in many arid regions, but differences can be observed in

those regions during rare precipitation events.

288

289

Figure 2: Quantile-quantile plot for the Central American land area for May 6, 2015-May 5,

2015. 100,000 quantiles (open circles) were calculated for the TMPA-RT and IMERG-L rainfall

estimates. In quantile mapping, a value from one product is used to look up the value of the

293   *second product at the same quantile. For example, if a TMPA-RT precipitation threshold were*

294   *180 mm day^{-1}, the equivalent IMERG-L value would be 231 mm day^{-1}.*
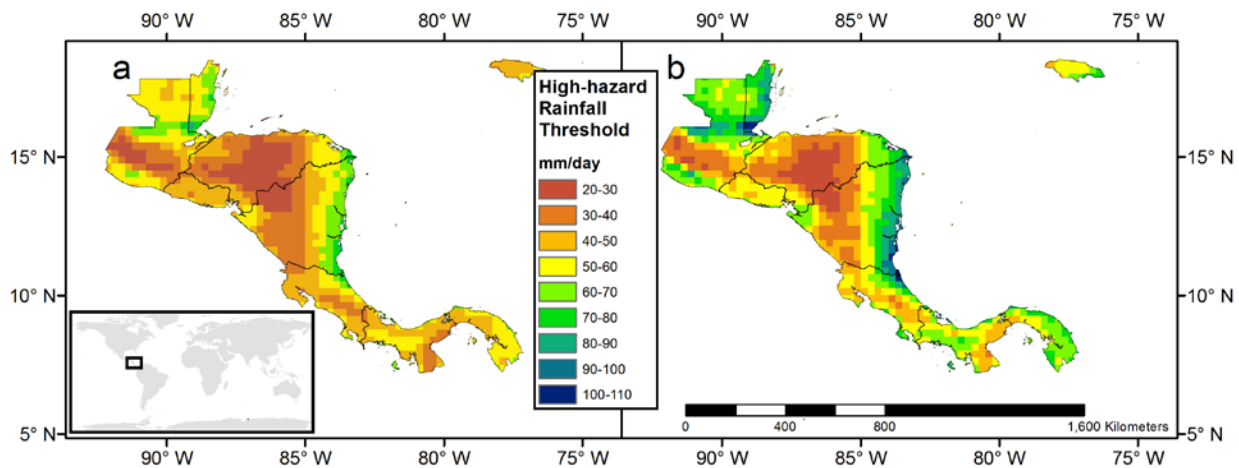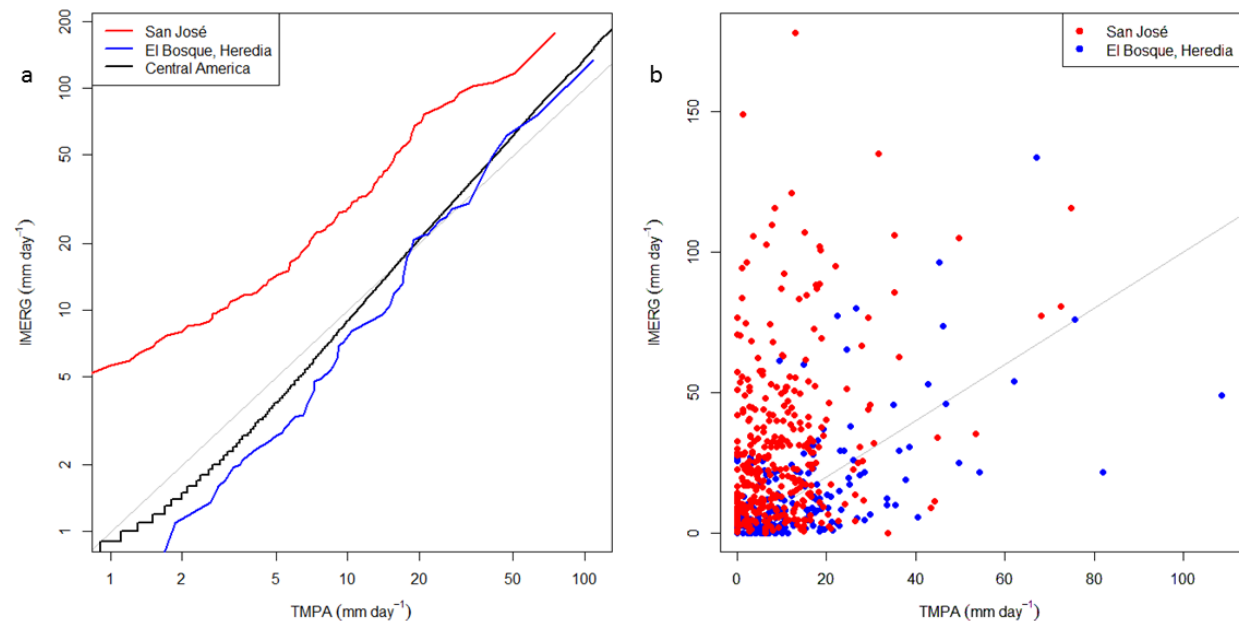
295

296

297   *Figure 3: The LHASA high-hazard rainfall threshold was calculated from a) TMPA-RT data for the*

298   *period 2001-2014, b) the quantile-mapped IMERG-L equivalent thresholds.*

299

300

301   *Figure 4: a) Quantile-quantile plot of two locations in Costa Rica, as well as the whole of Central*

302   *America (black). Dry days are not shown. El Bosque (blue) is separated from San José (red) by*

303   *approximately 45 kilometers, but the observed relationship between IMERG-L and TMPA-RT is*

304   *dramatically different. b) The capital of Costa Rica has an anomalous IMERG record, in which*

305   *precipitation is both heavier and more frequent.*